Visual appearance of a Morris–Thorne-wormhole

Thomas Müller[a)]
Institut für Astronomie und Astrophysik, Abteilung Theoretische Astrophysik, Auf der Morgenstelle 10, 72076 Tübingen, Germany

(Received 6 November 2003; accepted 2 April 2004)

Following the paper of Morris and Thorne on wormholes as a tool for teaching general relativity, we present the visual appearance of this simple spacetime using an embedding diagram and a raytracing program. Even if such a wormhole is not physically reasonable, we take the risk and take a short trip to an unreasonable parallel universe. © *2004 American Association of Physics Teachers.*
[DOI: 10.1119/1.1758220]

I. INTRODUCTION

If we wanted to leave our home planet, Earth, today and set out for new worlds, it would be a long and strenuous journey. Even a flight to Mars would take at least six months. But science fiction offers us a totally different possibility. For example with a ''warp-drive,'' we could simply overcome the light barrier by compressing the space between us and our destination and thus shorten the distance. A much more elegant way would be a shortcut in spacetime itself—a wormhole. In the film *Contact* which is based on Carl Sagan's novel[1] of the same name, the protagonist Dr. Eleanor Arroway overcomes any distance within a few instants of time by traveling through a wormhole. Indeed, Morris and Thorne[2] found a solution of Einstein's general relativity theory that represents a ''tunnel'' in spacetime and could in principle be traversed by human beings. But, unfortunately, it needs exotic matter for its generation.

We will assume that all exotic matter is transparent and does not interact with the observer. This Morris–Thorne (MT) wormhole can be described by a very simple metric, Eq. (1). However, it is not so easy to understand what an observer traveling in the corresponding spacetime would actually see. Until now, the spacetime of a wormhole has been illustrated only by its embedding diagram, which can lead to confusion. In this article we try to understand the structure of the MT wormhole spacetime by examining its embedding diagram together with the real visual appearance for an observer generated by four-dimensional raytracing. Detailed discussions about the physics of wormholes and their different shapes can be found in Visser.[3] We recommend Ref. 2 for a short introduction to wormhole geometries and their traversability.

The physical contents of the MT wormhole is reviewed in Sec. II. A helpful tool for understanding its geometry—especially for tracing null or timelike geodesics—is an embedding diagram as discussed in Sec. III. A qualitative description of photon orbits depending on an effective potential is given in Sec. IV. In Sec. V we will have a look at some of the crucial details of the raytracing system *RayViS*, and we will discuss the visual appearance of a MT wormhole in Sec. VI.

II. REVIEW OF PHYSICAL DETAILS

Morris and Thorne presented a very simple kind of wormhole in their 1988 paper.[2] The spacetime of this wormhole is described by the spherically symmetric and static metric

$$ds^2 = -dt^2 + dl^2 + (b_0^2 + l^2)(d\vartheta^2 + \sin^2\vartheta\, d\varphi^2), \tag{1}$$

where here and in the following geometric units ($G=c=1$) are used. The coordinate $l \in (-\infty, \infty)$ measures the proper radial distance at fixed t. Both limits of l represent an asymptotically flat region. The time coordinate t represents global time.

To fix an event in this spacetime, there is a natural choice of basis vectors

$$\mathbf{e}_t = \partial_t, \quad \mathbf{e}_l = \partial_l, \quad \mathbf{e}_\vartheta = \partial_\vartheta, \quad \mathbf{e}_\varphi = \partial_\varphi, \tag{2}$$

where the partial derivative operators $\partial_\mu (\mu = t, r, \vartheta, \varphi)$ represent the tangent vectors along the curve with constant coordinates $\nu (\nu \neq \mu)$ (see Fig. 1). A detailed description of this notation can be found in Ref. 4.

Next, we turn to the local frame of a static observer $(\mathbf{e}_{\hat{t}}, \mathbf{e}_{\hat{l}}, \mathbf{e}_{\hat{\vartheta}}, \mathbf{e}_{\hat{\varphi}})$ with

$$\mathbf{e}_{\hat{t}} = \partial_t, \quad \mathbf{e}_{\hat{l}} = \partial_l, \tag{3a}$$

$$\mathbf{e}_{\hat{\vartheta}} = \frac{1}{\sqrt{b_0^2 + l^2}}\partial_\vartheta, \quad \mathbf{e}_{\hat{\varphi}} = \frac{1}{\sqrt{b_0^2 + l^2}\sin\vartheta}\partial_\varphi. \tag{3b}$$

The Riemann curvature tensor in this local frame has only one independent component

$$R_{\hat{l}\hat{\vartheta}\hat{l}\hat{\vartheta}} = R_{\hat{l}\hat{\varphi}\hat{l}\hat{\varphi}} = -R_{\hat{\vartheta}\hat{\varphi}\hat{\vartheta}\hat{\varphi}} = -\frac{b_0^2}{(b_0^2 + l^2)^2}. \tag{4}$$

The only nonzero component of the Ricci tensor is $R_{\hat{l}\hat{l}} = -2b_0^2/(b_0^2 + l^2)^2$. Thus, the Einstein tensor reads

$$G_{\hat{t}\hat{t}} = G_{\hat{l}\hat{l}} = -G_{\hat{\vartheta}\hat{\vartheta}} = -G_{\hat{\varphi}\hat{\varphi}} = -\frac{b_0^2}{(b_0^2 + l^2)^2}. \tag{5}$$

Because all tensors are expressed with respect to the local frame, the components of the stress energy tensor deduced from the Einstein equations have direct physical interpretations: $T_{\hat{t}\hat{t}} = \rho(l)$ is the total energy density; $T_{\hat{l}\hat{l}} = -\tau(l)$ represents the tension per unit area in the radial direction; and $T_{\hat{\vartheta}\hat{\vartheta}} = T_{\hat{\varphi}\hat{\varphi}} = p(l)$ is the pressure in transverse direction. The annoying fact that the energy density is negative destroys one's hope of using this wormhole as a shortcut for space travels in the near future. Nevertheless, it is an interesting model for studying the visual appearance of a wormhole, because more realistic ones do not essentially differ from this one.

III. EMBEDDING DIAGRAM REVIEWED

We have no idea what a four-dimensional spacetime like the MT wormhole looks like. One way for visualizing the

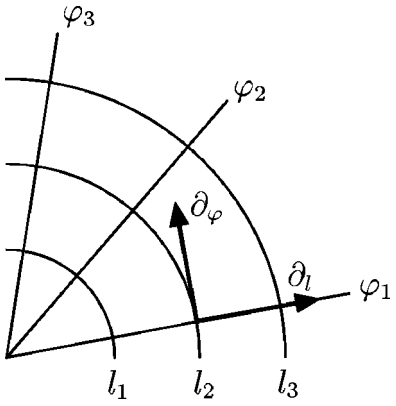

Fig. 1. Base vectors ∂_l and ∂_φ for the two-dimensional case.

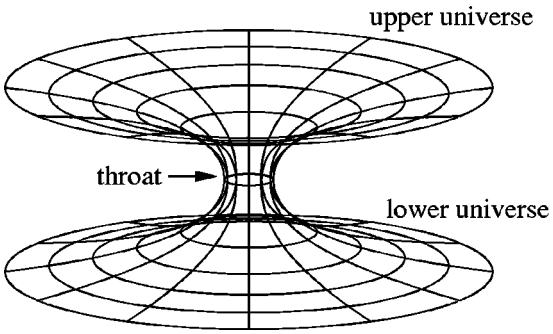

Fig. 2. 2-surface ($\vartheta=\pi/2$, $t=$constant) of the MT wormhole embedded in a Euclidean space.

inner geometry of a n-dimensional hypersurface is to embed it into a Euclidean $(n+1)$-dimensional surrounding space. The aim is to find a surface in the higher dimensional space that has the same inner geometry as the spacetime hypersurface. The embedding space has no physical meaning, however. So for example we can visualize the curvature of the surface of our home planet by embedding it in the three-dimensional space.

To understand the geometry of the MT wormhole, we can take advantage of the spherical symmetry and static nature of the metric and study only the equatorial "plane" at $\vartheta=\pi/2$ at a fixed instant of time. With the coordinate transformation $r^2=b_0^2+l^2$ the metric on this plane reads

$$d\sigma^2_{\text{2-surface}}=\frac{1}{(1-b_0^2/r^2)}dr^2+r^2d\varphi^2. \tag{6}$$

We can embed this two-surface in a three-dimensional Euclidean space, which is represented by cylindrical coordinates (r,φ,z), by identifying this surface with a surface $z=z(r)$. The metric of the surface in Euclidean space can be written as

$$d\sigma^2_{\text{euclidean}}=\left[1+\left(\frac{dz}{dr}\right)^2\right]dr^2+r^2d\varphi^2. \tag{7}$$

The comparison of Eq. (6) with Eq. (7) and integration with respect to r leads to the shape of the embedding diagram

$$z(r)=\pm b_0\ln\left[\frac{r}{b_0}+\sqrt{\left(\frac{r}{b_0}\right)^2-1}\right], \tag{8}$$

shown in Fig. 2. It is stressed that only the surface is part of the spacetime. The embedding space itself has no physical meaning. The impression of a tube as Fig. 2 might suggest is misleading. There is no tube in the spacetime, because the regions with radial coordinate $r<b_0$ are not part of the spacetime. The throat itself has a spherical topology and becomes important only for geodesics spiralling in, like water in a syphon. The qualitative behavior of null geodesics will be discussed in the following section. Their traces in an embedding diagram are shown in Sec. VI.

IV. PHOTON ORBITS

To analyze the behavior of geodesics, we will use the Lagrangian formalism (see Ref. 5 for a detailed discussion). A geodesic between two given points A and B satisfies the variational principle

$$0=\delta\int ds=\delta\int L d\lambda, \tag{9}$$

with the Lagrangian $L=\sqrt{|g_{\mu\nu}\dot{x}^\mu\dot{x}^\nu|}$. A dot means differentiation with respect to an affine parameter λ. Instead of solving the variational problem (9), we can consider an equivalent one, where

$$0=\delta\int \mathcal{L}d\lambda, \tag{10}$$

with $\mathcal{L}=L^2$, which also is valid for null geodesics. Here the Lagrangian $\mathcal{L}$ is defined by

$$\mathcal{L}=g_{\mu\nu}\dot{x}^\mu\dot{x}^\nu. \tag{11}$$

The geodesic equations follow from the Euler–Lagrangian equations

$$\frac{d}{d\lambda}\frac{\partial\mathcal{L}}{\partial\dot{x}^\mu}-\frac{\partial\mathcal{L}}{\partial x^\mu}=0. \tag{12}$$

As in Sec. III, we can take advantage of spherical symmetry. Thus, it will suffice to consider only null geodesics in the equatorial plane ($\vartheta=\pi/2$). It always is possible to rotate the coordinate system such that a null geodesic will lie completely in the equatorial plane. With $x^\mu=(t,l,\vartheta,\varphi)$ and Eq. (11), we have

$$\mathcal{L}_{mt}=-\dot{t}^2+\dot{l}^2+(b_0^2+l^2)\dot{\varphi}^2. \tag{13}$$

If we solve the Euler–Lagrangian Eqs. (12) for $\mu=t$ and $\mu=\varphi$, we find two constants of motion, $k=\dot{t}$ and $h=(b_0^2+l^2)\dot{\varphi}$, whose ratio $b=h/k$ is the apparent impact parameter. In particular, $b=0$ for radial curves. (Compare Ref. 4 for the Schwarzschild case.) Instead of solving the geodesic equations directly, we use the fact that $\mathcal{L}=0$ for null geodesics. If we use the constants of motion and Eq. (13), we get something like an *energy balance*

$$\dot{l}^2+V_p=k^2, \tag{14}$$

where $V_p=h^2/(b_0^2+l^2)$ is an effective potential for the light ray (see Fig. 3). Null geodesics with a constant $k<h/b_0(b>b_0)$ remain in the universe where they have been emitted.

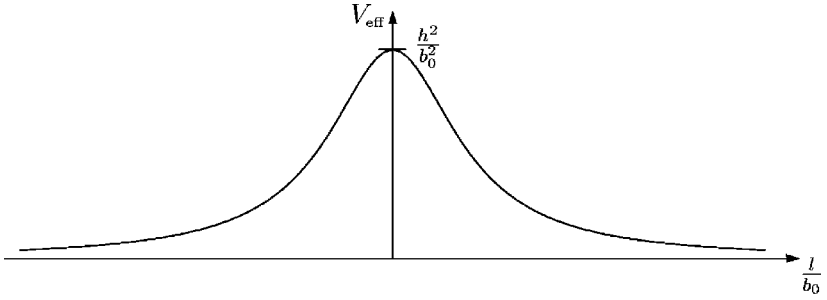

Fig. 3. Effective potential of a photon with angular momentum h in the MT wormhole spacetime.

They cannot overcome the angular momentum barrier. The ones with $k>h/b_0 (b<b_0)$ tunnel through the wormhole into the other universe. In the limiting case $k=h/b_0 (b=b_0)$, the null geodesic asymptotically approaches the throat.

From the point of view of raytracing, we can separate these three cases by the angle τ between the incoming/outgoing light ray and the radial direction to the wormhole with respect to a local observer (see Fig. 4). We directly see that

$$\sin^2\tau=\frac{(b_0^2+l^2)d\varphi^2}{dl^2+(b_0^2+l^2)d\varphi^2}=\frac{b_0^2+l^2}{b_0^2+l^2+(dl/d\varphi)^2}. \tag{15}$$

The derivative $dl/d\varphi$ can be substituted by

$$\left(\frac{dl}{d\varphi}\right)^2=\left(\frac{\dot{l}}{\dot{\varphi}}\right)^2=\frac{1}{b^2}(b_0^2+l^2)^2-(b_0^2+l^2), \tag{16}$$

which results from $\dot{l}=(dl/d\varphi)\dot{\varphi}$ and the Lagrangian equations. Thus, Eq. (15) becomes

$$\sin^2\tau=\frac{b^2}{b_0^2+l^2}, \tag{17}$$

with the critical angle $\tau_{\text{crit}}=\arcsin(b_0/\sqrt{b_0^2+l^2})$. Observers can now distinguish between light rays coming from their own universe ($\tau>\tau_{\text{crit}}$) or the other universe ($\tau<\tau_{\text{crit}}$) by measuring the incident angle τ.

Thus, we expect two regions for the visual appearance of a MT wormhole. The outer one—corresponding to $\tau>\tau_{\text{crit}}$—shows only the universe of the observer and the inner one is a window to the other universe.

V. VISUALIZING SYSTEM

The visualization of spacetimes can be done by four-dimensional raytracing. The figures in this article are rendered by the raytracing system *RayViS* developed by Gröne[6] and extended for four-dimensional raytracing by Weiskopf[7] and the author.[8]

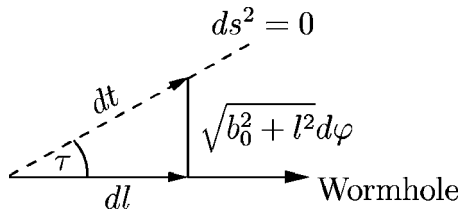

Fig. 4. Angle τ between the light ray ($ds^2=0$) and the radial direction to the wormhole.

A raytracing program is ideally suited for an object oriented approach (*RayViS* is implemented in C++). Three of its main components are the camera module, the ray-generating module, and the scenegraph. The camera represents the observer from which light rays (null geodesics) are traced back in time. For every pixel of an image the ray-generator calculates a light ray and passes it to the scenegraph, which determines its intersection with each object of the scenery.

In detail, null geodesics are implemented as piecewise linear curves. They are determined by integrating the null geodesic equation

$$\ddot{x}^\alpha+\Gamma^\alpha_{\beta\gamma}\dot{x}^\beta\dot{x}^\gamma=0, \quad \left(\dot{x}^\alpha=\frac{dx^\alpha}{d\lambda}\right) \tag{18}$$

from the spacetime point of the observer back to the spacetime point of emission. This integration is done by a fourth-order Runge–Kutta method. Stepsize control[9] is incorporated to take into account that spacetime has different curvature in different regions and for faster and more precise calculations. Initial values for the integration of a null geodesic are obtained from the camera module whose position is given in the coordinate reference system (t,l,ϑ,φ). The orientation of the camera—the direction of view **d**, the right-vector **r**, and the up-vector **u**—is given with respect to its local frame [Eqs. (3a)–(3b)]:

$$\mathbf{d}=d_l\mathbf{e}_{\hat{l}}+d_\vartheta\mathbf{e}_{\hat{\vartheta}}+d_\varphi\mathbf{e}_{\hat{\varphi}}, \tag{19a}$$

$$\mathbf{r}=r_l\mathbf{e}_{\hat{l}}+r_\vartheta\mathbf{e}_{\hat{\vartheta}}+r_\varphi\mathbf{e}_{\hat{\varphi}}, \tag{19b}$$

$$\mathbf{u}=u_l\mathbf{e}_{\hat{l}}+u_\vartheta\mathbf{e}_{\hat{\vartheta}}+u_\varphi\mathbf{e}_{\hat{\varphi}}, \tag{19c}$$

with $|\mathbf{d}|=|\mathbf{r}|=|\mathbf{u}|=1$ and $\mathbf{d}\times\mathbf{u}=\mathbf{r}$ (see Fig. 5).

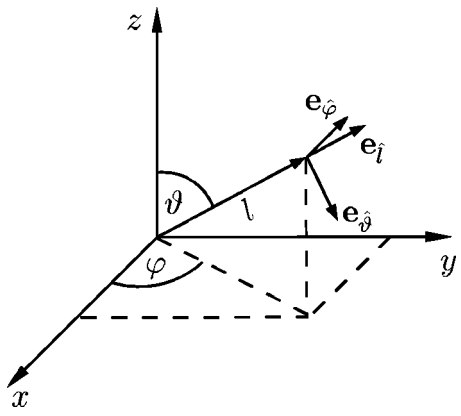

Fig. 5. The position of the camera is given by the spherical coordinates (l,ϑ,φ), whereas the orientation of the camera is given with respect to its local frame $(\mathbf{e}_{\hat{l}},\mathbf{e}_{\hat{\vartheta}},\mathbf{e}_{\hat{\varphi}})$.

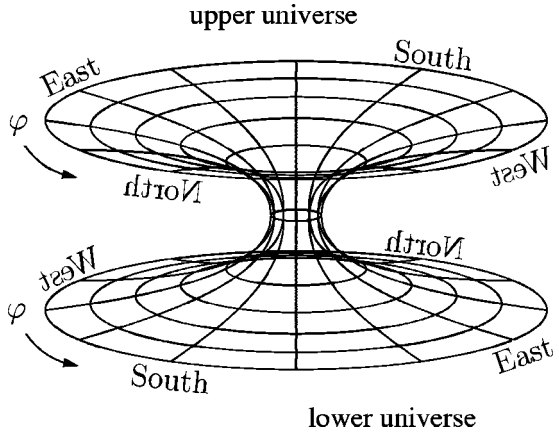

Fig. 6. Layout of the scenery illustrated in the embedding diagram.

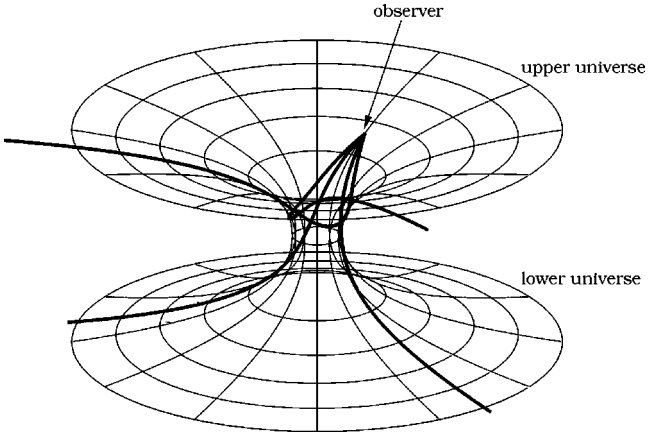

Fig. 8. Light rays in the embedding diagram that are responsible for the mirror images.

An initial direction **y** of a null geodesic as seen by the camera is thus

$$\mathbf{y}=y_1\mathbf{d}+y_2\mathbf{r}+y_3\mathbf{u}=\tilde{y}_1\partial_l+\tilde{y}_2\partial_\vartheta+\tilde{y}_3\partial_\varphi, \tag{20}$$

where $\tilde{y}_i$ are the initial values $\dot{x}^i(\lambda=0)$ for solving the null geodesic Eq. (18). The missing time component $\tilde{y}_0$ of the null direction has to be calculated from the null geodesic condition $g_{\mu\nu}\tilde{y}^\mu\tilde{y}^\nu=0$.

The next step is to intersect the null geodesics with the objects of the scenery which are all static. Rendering complex sceneries with high resolution needs a lot of computer resources. Because null geodesics do not interact, one can easily split the image into several parts which can be calculated on multiple processor computers.[10] Each segment of the light ray has to be intersected with all objects of the scenery. A more intelligent strategy is to divide spacetime into small volume elements, called voxels. Because we have a static scenery, it suffices to construct a three-dimensional spacelike grid. Every voxel stores all objects that lie completely or at least partially in it. To determine the voxels that are traversed by a light ray, we have to check the positions of all endpoints of the line segments relative to the grid. Hence, we have to intersect the light ray only with the non-empty voxels on the path of the light ray.

VI. VISUAL APPEARANCE

Contrary to the usual visualization of wormholes in science fiction films or in popular literature, one does not see a tube through which a spacecraft could travel. Neither strange light within the wormhole throat nor the possibility of looking into a surrounding space exists. Instead, the wormhole throat acts as a strange mirror showing our own and the other universe in a multiple way. We will check this effect by means of a simple model. To this end we will first represent the layout of the scenery and will then explain in detail what we see.

The Scenery. In the universe of the observer there is a regular lattice structure surrounding one side of the wormhole throat. Around the lattice there are signs showing the four directions of the compass, also called cardinal points. In the ''lower'' universe there is the same lattice structure also surrounded by four signs showing cardinal points. The crucial question is, how shall we position these signs? Here we have chosen the situation illustrated in Fig. 6.

Imagine that you start from the south in the ''upper'' universe and head strictly north. Then you will end up in the north of the lower universe. To have the same situation regardless of where you begin, we have to arrange the signs showing the main directions as we did in Fig. 6. Strictly speaking, if we put a sign, which shows the name of the direction to which we will walk in front of us in our local frame, then we must parallel transport our system to the other universe. After transportation we should be able to read both signs from left to right.

What we see. As long as the wormhole throat of radius $b_0=0$, we see only our own universe (Fig. 9). But if there is

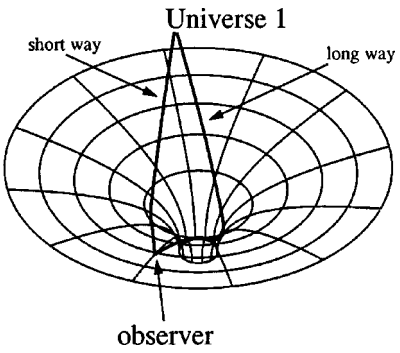

Fig. 7. Two light rays starting from the same point follow different light paths. (Here only the embedding diagram of the upper universe is drawn.)

Fig. 9. Lattice structure without a wormhole. The observer is located at $l=13,\vartheta=\pi/2,\varphi=\pi/2$. The camera has a field of view of $45°\times36°$.

Fig. 10. MT wormhole with throat radius $b_0=0.3$. The observer has the same position as in Fig. 9. But the field of view is reduced to $22.5°\times18°$ to focus on the distortion of the Universe North sign.

a wormhole throat of radius $b_0=0.3$ (Fig. 10), the lattice starts to distort slightly. Remember that the throat is in the middle of the lattice structure and thus is directly in front of us. The ''Universe North'' sign can be read twice. The appearance of these two images can be understood by following two light rays starting from the same point (for example, ''U'' in Fig. 7). One of them will take the direct path to the observer, which results in the slightly bended outer image, whereas the other one traverses the longer way around the throat and produces the mirrored inner image.

To have a better view of the inner environment, we stretch the throat to radius $b_0=2.0$ (Fig. 11). The lattice in our own universe seems a little bit more distorted. But the Universe North sign is now hardly readable because of the strong bending of light by the wormhole throat. Adjacent to the center, we can see the first mirror image of the complete lattice in our universe and closer to the center also the first mirror image of the other universe. Looking straight into the wormhole offers a view of the whole lattice of the lower universe. A bit more impressive is Fig. 12, where we have the same situation except that the wormhole throat is now surrounded by a textured, cubic room on each side. Here it becomes more obvious that we can see the complete room of the other universe through the wormhole.

To understand why we see mirror images within the throat, we have to follow light rays in the embedding diagram which pass close to or go through the throat (Fig. 8). If our camera has, for example, a horizontal field of view of 60°, we have to scan from $\tau=-30°$ to $\tau=30°$. Light rays with $\tau>\tau_{\text{crit}}$ [Eq. (17)] stay in our universe, but as we approach the critical angle, they will orbit around the throat. Hence, we not only see a distorted image of what is behind the wormhole throat, but also a mirror image of our near environment. After crossing the critical angle, the light ray orbits the throat before reaching the lattice or the walls of the room. Thus, we see a mirror image before we see the complete lattice or room of the other universe.

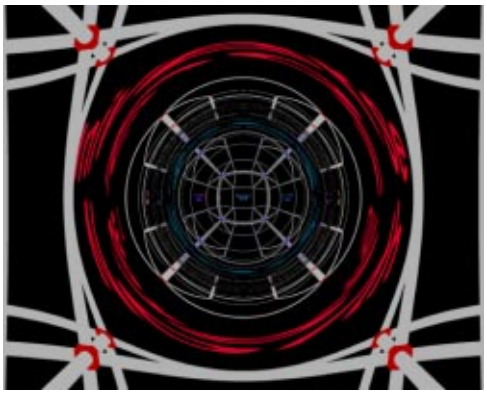

Fig. 11. MT wormhole with throat radius $b_0=2.0$. Note that the wormhole mouth is in the middle of the lattice structure in both universes. The critical angle mentioned in Sec. IV is $\tau_{\text{crit}}\approx8.7°$.

Fig. 12. Same situation as in Fig. 11. Now the wormhole throat is surrounded by a cubic room on each side, composed of floor, ceiling, and wall textures. (Upper: upper universe, Lower: lower universe.) The mirror images of both rooms can easily be seen in the throat of the wormhole. Note that one can see the complete room of the other universe.

ACKNOWLEDGMENTS

The author would like to thank Professor Dr. Hanns Ruder for the idea of this work and P.D. Dr. Jörg Frauendiener for many discussions and for carefully reading the manuscript. This work was supported by the Deutsche Forschungsgesellschaft (DFG), SFB 382, Teilprojekt D4.

[a]Electronic mail: tmueller@tat.physik.uni-tuebingen.de; URL: www.tat.physik.uni-tuebingen.de/~scri

[1]Carl Sagan, *Contact* (Simon and Schuster, New York, 1985).

[2]Micheal S. Morris and Kip S. Thorne, ''Wormholes in spacetime and their use for interstellar travel: A tool for teaching general relativity,'' Am. J. Phys. **56**, 395–412 (1988).

[3]Matt Visser, *Lorentzian Wormholes: From Einstein to Hawking* (AIP, Woodbury, NY, 1995).
[4]C. W. Misner, K. S. Thorne, and J. A. Wheeler, *Gravitation* (W. H. Freeman, New York, 1973).
[5]Wolfgang Rindler, *Relativity–Special, General and Cosmology* (Oxford University Press, New York, 2001).
[6]Alwin Gröne, ''Entwurf eines objektorientierten Visualisierungssystems auf der Basis von Raytracing,'' Ph.D. thesis, Eberhard-Karls-Universität Tübingen, 1996.
[7]Daniel Weiskopf, ''Visualization of four-dimensional spacetimes,'' Ph.D. thesis, Eberhard-Karls-Universität Tübingen, 2001.
[8]See EPAPS Document No. E-AJPIAS-72-011407, for accompanying color figures and small animations. A direct link to this document may be found in the online article's HTML reference section. The document may also be reached via the EPAPS homepage (http://www.aip.org/pubservs/epaps.html) or from ftp.aip.org in the directory /epaps. See the EPAPS homepage for more information.
[9]W. H. Press, S. A. Teukolsky, W. T. Vetterling, and B. P. Flannery, *Numerical Recipes in C* (Cambridge U.P., Cambridge, 1992).
[10]Kepler-Cluster computer, ⟨http://kepler.sfb382-zdv.uni-tuebingen.de/kepler/⟩.

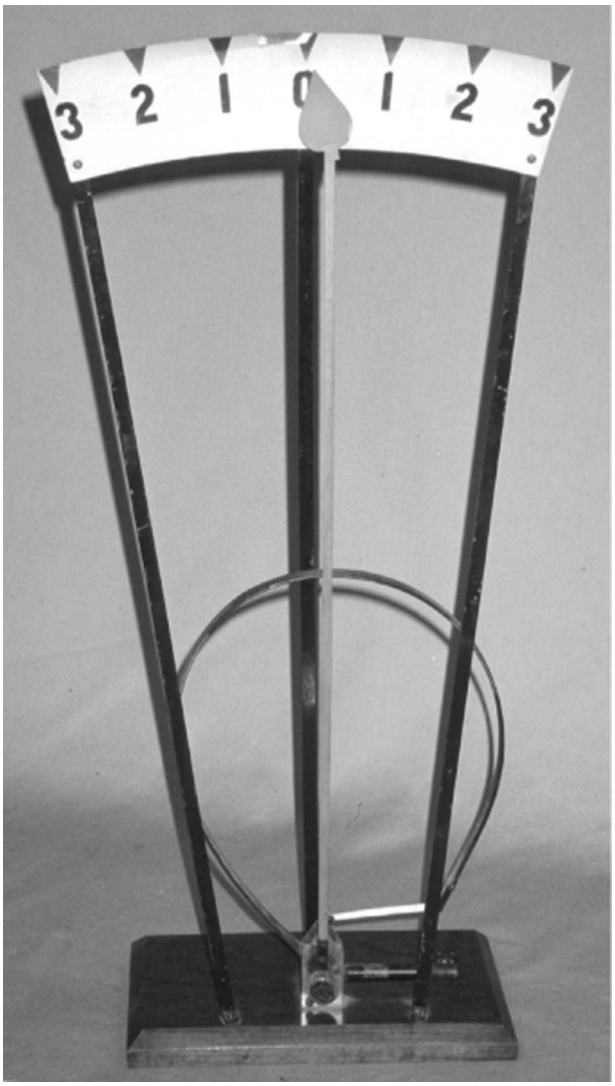

Bourdon Tube. The only absolute pressure gauge is the manometer, but, because it is liquid filled, it is difficult to transport, and must always be kept vertical. The Bourdon tube pressure gauge, invented in France in 1849 by Eugene Bourdon, must be calibrated using known pressures. In this design the gas whose pressure is to be measured is introduced into a flattened tube coiled into a full circle. As the pressure increases the tube straightens out, and the motion of the free end of the tube is amplified by a mechanical level mechanism. The apparatus is in the Cornell University collection of demonstration apparatus, and is large enough to be viewed by a class of several hundred students. (Photograph and notes by Thomas B. Greenslade, Jr., Kenyon College)